Micron 170 (2023) 103460

Contents lists available at ScienceDirect

Micron

journal homepage: www.elsevier.com/locate/micron

Progress in the applications of atomic force microscope (AFM) for mineralogical research

Qin Liu [a], Yuhong Fu [a,*], Zonghua Qin [b], Yun Wang [a], Shanshan Zhang [a], Meimei Ran [a]

[a] School of Geography & Environmental Science, Guizhou Normal University, Guiyang, Guizhou 550025, China
[b] State Key Laboratory of Ore Deposit Geochemistry, Institute of Geochemistry, Chinese Academy of Sciences, Guiyang, Guizhou 550081, China

ARTICLE INFO

Keywords:
Atomic force microscope
Mineral
Mineral-aqueous interfaces
Surface properties

ABSTRACT

Mineral surface properties and mineral-aqueous interfacial reactions are essential factors affecting the geochemical cycle, related environmental impacts, and bioavailability of chemical elements. Compared to macroscopic analytical instruments, an atomic force microscope (AFM) provides necessary and vital information for analyzing mineral structure, especially the mineral-aqueous interfaces, and has excellent application prospects in mineralogical research. This paper presents recent advances in the study of properties of minerals such as surface roughness, crystal structure and adhesion by atomic force microscopy, as well as the progress of application and main contributions in mineral-aqueous interfaces analysis, such as mineral dissolution, redox and adsorption processes. It describes the principles, range of applications, strengths and weaknesses of using AFM in combination with IR and Raman spectroscopy instruments to characterization of minerals. Finally, according to the limitations of the AFM structure and function, this research proposes some ideas and suggestions for developing and designing AFM techniques.

1. Introduction

In the history of modern instrument development, the microscopic technique has continuously improved with the advancement of science and technology and has significantly contributed to microscopic research. For example, in 1982, Binnig and Rohrer (1982) developed a scanning tunneling microscope (STM) at the IBM Zurich Laboratory, which can use the current between the probe and the sample to characterize various physical, chemical, and mechanical properties of the sample's surface. It was the first time humans had directly observed the sample's arrangement sequence of individual atoms. Even in the environment of a low temperature of 4 K or a high temperature of 1000 K, the atoms can be accurately manipulated by the probe tip. However, STM can only directly observe the surface structure of metal conductors and semiconductors because the changes in tunnel current between the probe tip and the sample must be monitored when it works. When an insulation material is observed, it is necessary to cover a conductive film on its surface, but the structural details of the sample surface could be covered by it. As a result, the applications of STM are limited to a certain extent (Couto et al., 2006). Then in 1986, Binning from IBM, Quate and Gerber from Stanford University co-developed atomic force microscope (AFM) (Binnig et al., 1986). The arrival of AFM solves the limitation of STM that can only test conductor and semiconductor samples and realizes the manipulation and processing of the atomic structure of non-conductor samples (Gross et al., 2018). The AFM can in situ detect the crystal structure and degree of surface defect of conductor and non-conductor samples and observe the three-dimensional morphology of nano-scale samples in real-time. Also, AFM can be equipped with a fluid cell; in addition to studying solid samples, it can explore the surface reaction process of samples in a liquid environment (Feng et al., 2020; Tadesse et al., 2019). In addition, AFM can be utilized to investigate the acting forces on the samples' surface. Due to its broad application scenarios and simple sample preparation process, AFM has been widely used in many fields, including earth science, physics, materials science, biological science, and environmental science (Wang et al., 2021b; Fukuma and Garcia, 2018; Hong et al., 2020; Strahlendorff et al., 2019).

The AFM does not have any measuring lens, and its main structure consists of five components, including a cantilever, a probe tip, a laser photodiode system, a three-dimensional piezoelectric scanner, and a feedback controller (Zhu and Sun, 2005). The probe tip and cantilever constituting the core components of the instrument, which determine whether the high quality AFM images of samples can be obtained

* Corresponding author.
E-mail address: fuyuhong10@163.com (Y. Fu).

https://doi.org/10.1016/j.micron.2023.103460
Received 9 March 2023; Received in revised form 12 April 2023; Accepted 12 April 2023
Available online 20 April 2023

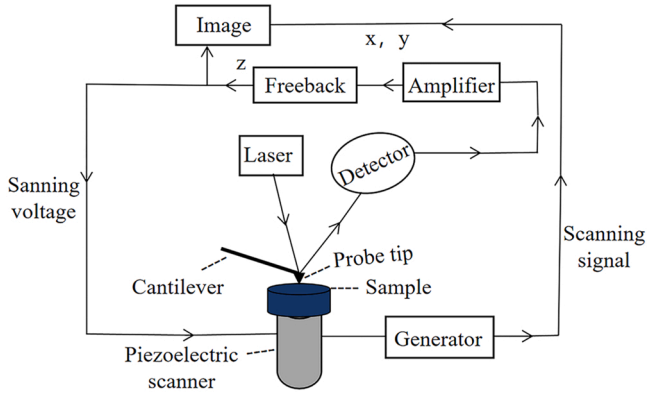

Fig. 1. Schematic diagram of AFM (Zhao et al., 2019). Copyright (2019), with permission from Elsevier.

(Fig. 1). During the imaging process, there is a very weak interaction between the probe tip and the sample surface, which deflects the cantilever of the probe, and the deflection of the cantilever deflects the reflected path of the irradiated laser. The detector converts and amplifies the reflected laser signal, and the feedback system adjusts the interaction between the probe tip and the sample surface by adjusting the distance between the two, while the signal acquisition system records the movement of the scanner in real time to obtain information about the sample surface (Hirsekorn et al., 1997; Sader et al., 2005; Stark, 2000). AFM is imaged by the probe on the surface of the samples. Some properties can be obtained by changing the interaction force between the probe and samples, include the atomic resolution morphology, wettability, adhesion and surface charge, etc. The use of magnetic probes can also detect the magnetic force distribution on the sample surface, etc (Bian et al., 2021). AFM can also detect the magnetic field force distribution on the sample's surface if a magnetic probe is employed. The AFM imaging modes consist primarily of tapping mode, contact mode, non-contact mode, torsional resonance mode, and peak force mode, with contact mode, non-contact mode, and tapping mode constituting the basic imaging modes of AFM (Vijayraghavan et al., 2013). Under the contact mode, the probe tip is directly in contact with the sample's surface, resulting in a higher imaging resolution. However, since the cantilever and probe tip are usually silicon nitride, the force between the probe and the sample should be adequately controlled to avoid damaging the probe when handling samples with too high hardness (Xing et al., 2018; Kolchuzhin et al., 2016). Under the non-contact mode, the probe tip does not directly contact the sample's surface but generates the sample's surface morphological images through the interactions of capillary pressure or van der Waals forces between the probe tip and the sample surface (Alvim and Miranda, 2016). The cantilever is bent due to the interaction between the sample's surface and the probe tip, and it is deflected as a result of the stress exerted, thus generating the image of the sample surface as a feedback loop (Shinato et al., 2020; Zhang et al., 2018; Sokolov et al., 2000). Under the tapping mode, the cantilever resonates under the drive of external force. The cantilever drives the probe back and forth across the force distance curve. The probe vibrates in both the long-range attractive and short-range repulsive regions of the force curve, but high-resolution imaging of the sample is usually in the short-range repulsive region of the force curve. Unlike the contact mode, the probe intermittently contacts the sample surface for short periods of time, thus avoiding the problems of lateral forces and drag across the surface, improving both the resolution of some samples with soft surfaces and the lifetime of the probe (Paulo and García, 2002; Hansma et al., 1994).

Minerals are an essential part of earth's evolution, which not only directly participate in the geological process of earth's evolution but also record important information about earth's evolution. In addition, mineral surface properties critically influence the geochemical cycle of related elements, ecological effects, and mineral exploitation and utilization (Zhang et al., 2019a; Xie and van Zyl, 2020). As one of the important instruments for studying mineral surface properties, AFM cannot only be utilized to detect the nano-scale three-dimensional morphology of mineral surfaces, mineral roughness, and mineral crystal structure (Toca-Herrera, 2019), but also provide powerful help for exploring the mineral-aqueous interfacial reactions. AFM has been widely applied in the research on ore weathering, production and treatment of acid mine wastewater, and migration and transformation of related pollutants (López et al., 2018; El-Nagar and Abdel-Halim, 2021). However, as far as we know, there are relatively few reviews on the application of AFM to mineral surfaces, the recent being a review of mineral surface research published in 2014 (Jupille, 2014). AFM has made some progress in mineralogy in recent years, so there is an urgent need to review the content and results of research on mineral surface properties. Accordingly, this study mainly reviews the research progress of using AFM to explore mineral surface properties and mineral-aqueous interfacial reactions in the past ten years, introduces the principles, strengths, and weaknesses of the combination of AFM with other spectral instruments, and puts forward some ideas and suggestions for the applications of AFM in the field of mineral research. It is believed that this work can provide some help for further promoting the research on mineral surface properties.

2. Applications of AFM in mineralogical research

2.1. Applications of AFM in researching mineral surface properties

2.1.1. Roughness

Surface roughness is one of the indices that reflect the shape characteristics of microcosmic geometry on mineral surfaces, and it is also an important parameter that affects the utilization rate of the mineral industry. Generally, with the increase in mineral roughness, the wettability of minerals becomes worse, and the flotation performance is enhanced (Li et al., 2019; Alnoush et al., 2021). In the mineral surface treatment and film manufacturing process, there are optical cutting methods (Perec et al., 2017), comparison methods (Fava et al., 2018), and white light interferometer (Deng et al., 2018), which can be utilized to treat and measure surface roughness. Compared to traditional methods, AFM can detect mineral surface roughness more intuitively (Misumi et al., 2019). By measuring the sample's three-dimensional surface roughness map, AFM can calculate the average roughness (R_a), root mean square roughness (R_q), surface skewness (R_{sk}), and surface kurtosis (R_{ku}) relying on the relevant parameters, such as amplitude threshold, scanning rate, and integral gain (Eqs. (1–4)). In this study, the transverse resolution of roughness can reach 0.1 nm, while the longitudinal resolution can achieve 0.01 nm (Gan, 2009).

Ra is the average difference between an individual's height and its mean (Abouelatta and Mádl, 2001). It is obtained from the arithmetic mean value of the absolute values of the surface height deviation measured on the sample plane (Chen and Huang, 2004; Chang et al., 2001), which can be calculated as follows:

$$R_a = \frac{1}{N_x N_y} \sum_{i=1}^{N_x} \sum_{j=1}^{N_Y} Z(i\ ,\ j) - Z_{mean} \tag{1}$$

$$Z_{mean} = \frac{1}{N_x N_y} \sum_{i=1}^{N_x} \sum_{J=1}^{N_y} Z(i\ ,\ j) \tag{2}$$

where N_x and N_y are the numbers of scanning points in the X and Y directions, respectively; Z(i , j) is the deviation values of the height; Z_{mean} is the average height of the baseline; the same below.

R_q is a commonly utilized parameter representing surface topography's standard deviation. It is obtained from the root mean square mean value of the height deviation values of the image data on the

sample plane, which can be calculated as follows:

$$R_q = \sqrt{\frac{1}{N_x N_y}\sum_{i=1}^{N_x}\sum_{j=1}^{N_y}(Z(i\ ,\ j) - Z_{mean})^2} \tag{3}$$

R_{sk} describes the symmetry of the surface height data distribution. If the value is zero, it indicates that the sample surface is smooth; if there are many peaks on the surface, it means positive asymmetry; if there are many deep depressions on the surface, it demonstrates negative asymmetry. The calculation formula is as follows:

$$R_{sk} = \frac{1}{N_x N_y R_q^3}\sum_{i=1}^{N_x}\sum_{j=1}^{N_y}(Z(i\ ,\ j) - Z_{mean})^3 \tag{4}$$

R_{ku} is the surface excessive kurtosis equal to zero under the normal distribution. When the surface data are more concentrated on the mean value as opposed to following a normal distribution, the kurtosis is positive; when they are not concentrated, the kurtosis is negative. The calculation formula is as follows:

$$R_{ku} = \frac{1}{N_x N_y R_q^4}\sum_{i=1}^{N_x}\sum_{j=1}^{N_y}(Z(i\ ,\ j) - Z_{mean})^4 - 3 \tag{5}$$

Through AFM observation, it is indicated that the treatments such as grinding and calcination can increase the roughness of mineral surfaces. For example, previous detections by AFM have shown that grinding treatment on graphite (Tong et al., 2021), quartz (Zhu et al., 2020c), magnesite (Zhu et al., 2020a), and magnetite (Zhu et al., 2020b) by ball, rod, and high-pressure roll mills can increase the minerals' surface roughness, which enhanced the flotation capacity of minerals. By using the method of hydrochloric acid leaching - precipitation - calcination, Altiner and Mahmut (Altiner, 2019) prepared MgO particles with different surface roughness from dolomite. They demonstrated that the surface roughness of the prepared MgO particles rose with the increase in calcination temperature and time, which improved the utilization rate of dolomite in industry. In addition, it is indicated that some chemical treatments can change the minerals' surface roughness. After fluoride ion treatment, the surface topography of calcite became more uneven, and the roughness increased significantly (Wang et al., 2022). Under the impact of hydrolytic products (H_2 and O_2), the surface of galena, chalcopyrite, and sphalerite became rougher; of course, this can also be attributed to the air oxidation effect in the polishing process, producing multiple scratches on the surface (Koporulina et al., 2018). Sun et al. (2022) found that adding calcium dioleate colloid will increase the surface roughness of scheelite and fluorite, and improve the flotation capacity of scheelite and fluorite. On the other hand, AFM also detects that some treatments can reduce the surface roughness of minerals. For example, after microwave irradiation, the surface roughness of chalcopyrite decreased and the wettability of the mineral surfaces enhanced (Azghdi and Barani, 2018). To sum up, the measurement precision of mineral surface roughness by AFM can achieve nanometer resolution, making AFM one of the first-choice instruments for measuring mineral surface roughness.

2.1.2. Crystal structure

With the help of crystal growth theory, mineral crystal models such as calcite in the tripartite crystal system and pyrite in the orthogonal crystal system have been developed, most of that are obtained from indirect analysis based on the theories, like crystal layer growth and crystal spiral growth (He et al., 2020). Although the transmission electron microscope (TEM) technique can directly observe the sample's crystal structure, it can cause irreversible damage to the sample due to the irradiation of electron beams. This problem was not solved until AFM's appearance (Liu et al., 2003). As early as the around 2000, some scholars employed AFM to observe the minerals' crystal structure, such as silicate and carbonate (Wu et al., 1998; Liu, 2003). In recent years, the applications of AFM to the research on mineral crystal structure have made some progress, including observing the dynamic process of the growth interface of mineral crystals and the atomic-resolution imaging of mineral interface in a liquid environment. The progress has essential theoretical and practical significance for developing crystal growth theories and guiding crystal production practice.

In the study of mineral crystal structure, the fine crystal structure and diverse types of clay minerals have been widely concerned. The common instruments and technical methods for investigating the surface composition and structure of clay minerals include low-energy electron diffractometer (LEED), scanning electron microscopy (SEM), X-ray photoelectron spectroscopy (XPS), and Derjaguin-Landau-Verwey-Overbeek (DLVO) theoretical calculation (Muneer et al., 2020). Due to the particular crystal structure of natural clay minerals, these methods have a certain limitation of insufficient spatial resolution when observing the zones of lattice defects and atomic steps on the sample surface. Fortunately, AFM has high resolution and can measure samples even in environments such as liquid and vacuum. During in-situ characterization of minerals, physical changes and chemical reactions, such as hole potential and electronic band gap at the defects on the minerals' surface, can be intuitively learned by AFM. For example, in the liquid environment of ultra-pure water, Siretanu et al. (2016) characterized the morphology and atomic structure of nano-scale clay minerals by AFM. They obtained atomic-resolution images (Fig. 2) of the (001) crystal face of bauxite, kaolinite, illite, and sodium montmorillonite minerals. It was observed that there were a large number of defects on the mineral surfaces and that some organic and inorganic substances were adsorbed on the minerals' surface defects in the water environment. However, the specific characteristics of these adsorbed substances are still unclear. Reischl et al. (2019) conducted an atomic molecular dynamics simulation of the structure and dynamics of the hydration layer on the surface of dolomite, calcite, and magnesite and performed AFM simulation imaging on the surface of these three minerals by SiO_2 tip model. In the process of atomic simulation, it was indicated that the AFM technique could distinguish Ca^{2+} and Mg^{2+} of dolomite. AFM can also achieve ion exchange on the mineral surfaces in a liquid environment, laying a foundation for AFM to detect the hydration structure of minerals. In addition, Zhai et al. (2021) examined the mineral crystal growth process by AFM based on dynamic force spectrum (DFS) technique, and enumerated the dynamic processes of mineral growth of the interfaces between alginate $(C_6H_8O_6)_n$ and hematite (Fe_2O_3), between natural organic matter (NOM) and calcium arsenate ($Ca_3(AsO_4)_2$), and between calcium phosphate ($Ca_3(PO_4)_2$) and hydroxyapatite (HAP). They revealed that the crystal nucleation rate, nucleus size, growth orientation, and structure of organically modified minerals improved the basic understanding of the interaction between organics and minerals, providing a reference value for investigating the crystal nucleation and growth in the process of biomineralization and geological mineralization. The research on the growth of clay minerals and mineral crystals by AFM has brought new impacts and challenges to the previous crystal structure models and theories, and some breakthroughs have been made in studying mineral crystal structure. In the future, the applications of the AFM technique in investigating mineral crystal structure will be more and more extensive.

2.1.3. Three-dimensional morphologies

The surface morphological characteristic images of the samples measured by AFM differ from those of other microscopes. For example, SEM and TEM have a higher resolution for imaging two-dimensional morphology on the sample surface, while AFM has a special probe to scan the sample, which can directly analyze the three-dimensional images of the sample surface. Therefore, the AFM's three-dimensional characterization performance for mineral morphology and particle size can be greatly improved. Bai et al., (2022) used AFM to characterize Muscovite for the first time and obtained two-dimensional (2D) images, three-dimensional (3D) structural images, and surface roughness of

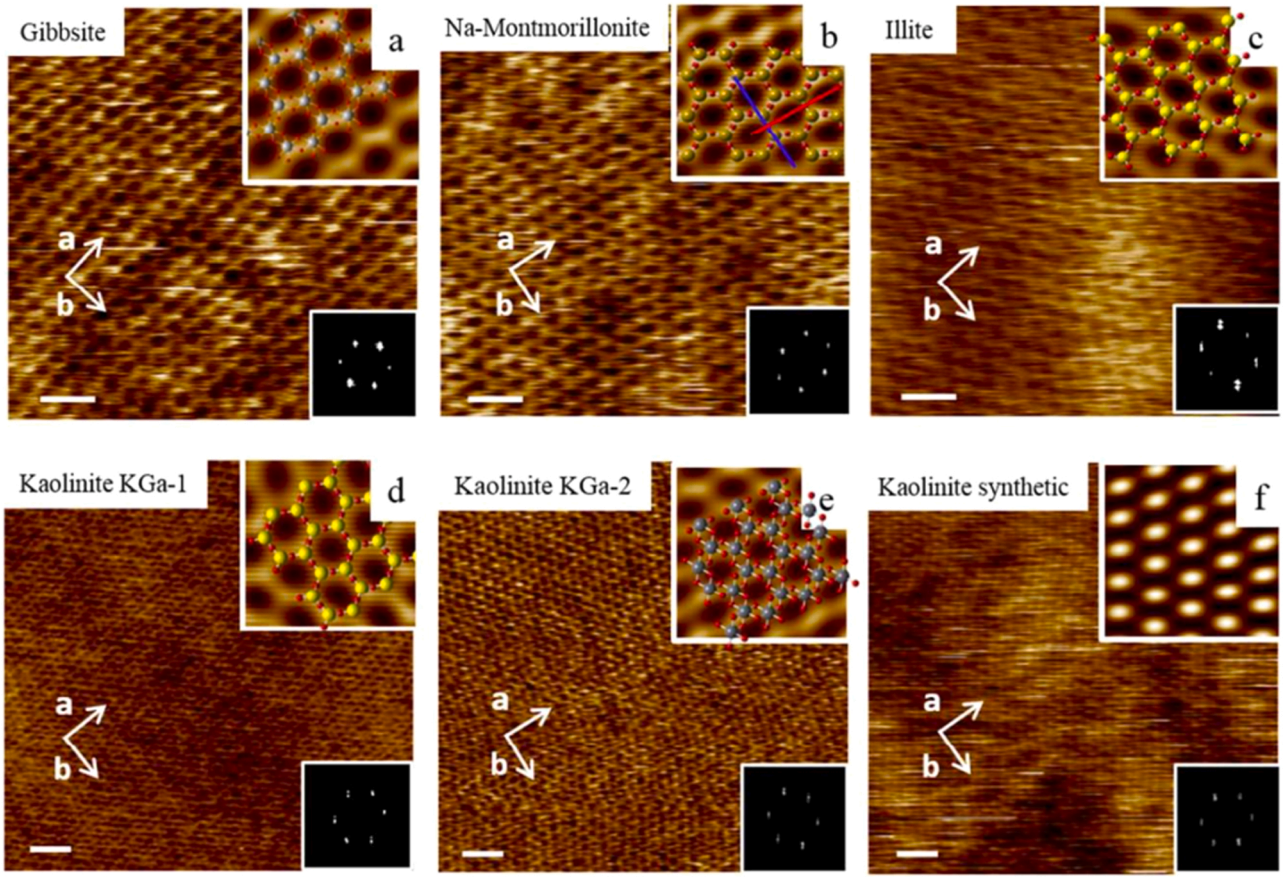

Fig. 2. Atomic-resolution AFM images on the clay cardinal plane: (a) gibbsite, (b) Na-Montmorillonite, and (c) illite; (d-f) high-resolution non-contacted AM-AFM morphological maps of the cardinal plane of kaolinite clay particles (when kaolinite clay is exposed in the ultra-pure water, it shows a periodic hexagonal structure, and the transverse period of the crystal lattice is about 0.5 nm (Siretanu et al., 2016)). Copyright (2016), with permission from Royal Society of Chemistry.

Muscovite (Fig. 3). Montmorillonite (MMT) is a two-dimensional nano-mineral whose structure is perceived in layers connected by cations (Na^+ and Ca^{2+}), which can be employed to adsorb dyes and heavy metal ions in water pollution treatment. Zhang et al. (2017b) examined MMT's morphology, thickness distribution, and particle size through 3D-AFM and found that Na-MMT is easier to exfoliate than Ca-MMT. This phenomenon was suggested to be attributed to the higher interlayer binding energy (IBE) of Ca-MMT or the weak interaction between MMT and the Na^+-water layer. Hence, Ca-MMT had a better water pollution removal effect. Ismail et al. (2020) treated HAP by laser and observed the surface changes of minerals using 3D-AFM. They demonstrated that there are very fine particles on the HAP surface without laser treatment, while spherical grains are uniformly distributed on the surface of HAP samples treated by laser with a power of 60 J/cm^2; moreover, the microhardness of HAP increases after laser treatment,

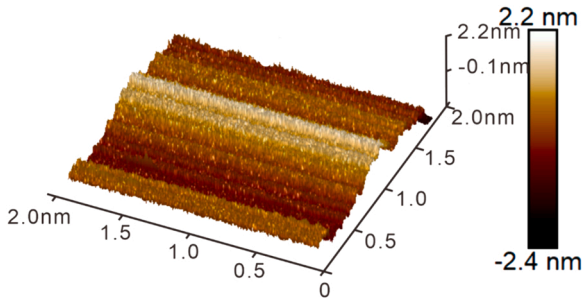

Fig. 3. AFM 3D height image structural image of the muscovite sample (Bai et al., 2022). Copyright (2022), with permission from MDPI.

improving the wear resistance (Garcia et al., 2016). So far, AFM is utilized to obtain atomic-resolution images of various substances, including insulators and conductors, e.g., layered minerals such as graphite, molybdenum disulfide (MoS_2), and boron nitride (BN). In addition, the 3D-AFM technique can provide intuitive characteristic images for characterizing the changes in the modified mineral surfaces, for example, whether there is an agglomeration phenomenon on the modified mineral surfaces or whether some new substances are formed. Moreover, the AFM 3D image technique can meet the measurement requirements in various atmospheres and environments, contributing to the mineral field and showing extensive application prospects in the materials preparation field.

2.1.4. Adhesion forces

The various forces exerted on the mineral surfaces can be measured using the instruments such as the surface force apparatus (SFA) (Zhang et al., 2012), micro-hardness tester (MHT) (Qudoos et al., 2018), and nano-indentor (Jin et al., 2015). There are also force interactions when the AFM technique is utilized to measure mineral surface properties, and the most common acting force is the van der Waals force. Due to the contact between the tip and the sample, the deformation force will be generated. If there is liquid, there will be surface tension. Sometimes, some special samples can produce magnetic force. Generally, the acting force, such as the electrostatic force and van der Waals force between the probe tip and the sample, is called the adhesion force. Using Lennard-Jones interaction to analyze the interaction between the atoms on the mineral surface and the tip of the probe, when the distance between the mineral sample and probe tip is less than $\delta(\delta \approx 0.3\text{nm}$, depends on the size of the sample atom), the adhesion force between the

mineral sample and probe tip is repulsive. If the distance between the mineral sample and the probe tip is more than $2(1/6)\delta$, the adhesion force between them is attractive (Muller and Derjaguin, 1980). Thus, when the probe tip touches and then leaves away from the sample, there will be a certain point with maximum attractive force on the force-distance curve. Depending on the measurement method, the adhesion force between the probe tip and the sample is also different. A colloidal probe technique usually measures the adhesion force, i.e., a small number of droplets or particles are fixed on the probe to determine the adhesion force between the probe tip and the sample. Abed et al. (2018) investigated the adhesion force on the carbonate surface by AFM colloidal probe technique under the force volume (FV) mode and drew the adhesion force diagrams between crude oil and natural mineral calcite and between crude oil and dolomite (Fig. 4). As can be seen, the adhesion force measured in the dolomite zone is at least twice that in the calcite zone, and dolomite areas are more oil-friendly than calcite areas. Due to the different composition of carbonate minerals, the adhesion and wettability of carbonate rocks are different, and the oil-affinity of minerals is also different. Tessarolo et al. (2021) used the AFM to explore carbonate rock oil reservoirs. Therefore, using AFM colloid probe to study the change of carbonate surface adhesion can provide an innovative method for oil reservoir development.

The salt solution type and concentration significantly influence the adhesion force between the probe tip and the mineral. Ding et al. 2020) modified the probe to explore the effects of salt solution (Ca^{2+}, Mg^{2+}, and Na^{+}) on the surface adhesion of calcite. By fixing the crude oil droplets on the cantilever without an AFM tip, they used the "soft tip" method to detect the changes in the surface adhesion of calcite in different salt solutions. Combing the force behavior of the adhesion force-distance curve and the adhesion values on the contraction curve revealed that the attractive force between the crude oil tip and calcite was strongest in the salt solution containing Mg^{2+}, then Na^{+}, and the weakest in the solution containing Ca^{2+}. Zou et al. (2020) studied the interaction force between the polymer and the surface of SiO_2 or Al_2O_3 in a KCl solution using the AFM colloidal probe technique. They discovered that the adhesion force between Al_2O_3 and the polymer decreased, while that between SiO_2 and the polymer increased as KCl concentration rose. Zhang et al. soaked the fluorite colloidal probe and the sample in $Ca(OH)_2$ solution for 30 min before each separation test of scheelite and fluorite, and the measurement results showed that $Ca(OH)_2$ solution will raise the hydrophilicity of scheelite and fluorite and lead to the increase in adhesion force between scheelite and fluorite. These findings provide good guidance for separating scheelite from other calcium-containing minerals (Zhang et al., 2019b).

In addition to the types of salt solution, the pH value of solution also affects the adhesion force between the probe tip and the mineral. Al Maskari et al. (2019) analyzed the adhesion force between petroleum and Muscovite rock based on the force-distance curve at pH = 7 and 11. They indicated that the lamella-charged Muscovite rock will increase the pH value due to ion exchange, decreasing adhesion force. In order to improve the quality of iron and steel smelted from iron ore pellets, Dobryden et al. (2014) used fine SiO_2 particles as a probe to contact magnetite (Fe_3O_4) and bentonite and tested the adhesion force of four systems, including SiO_2 and Fe_3O_4, Fe_3O_4 and Fe_3O_4, SiO_2 and bentonite, and Fe_3O_4 and bentonite. The adhesion force of the Fe_3O_4--bentonite system increases under alkaline conditions, whereas the SiO_2-Fe_3O_4 system decreases in the presence of SiO_2. Hence, the agglomeration of Fe_3O_4 and bentonite binder can be affected by SiO_2 particles on the Fe_3O_4 surface under alkaline conditions, which is not conducive to producing high-quality iron ore pellets. When studying the adhesion force between non-polar oil base (– CH_3) and calcite, Maskari et al. (2019) also indicated that the adhesion force between them reduces with the increase in pH value. Shao et al. (2019) used AFM force measurement and classical DLVO theory for the first time to investigate the interaction force between illite lamellae or end face and Si/Si_3N_4 probe in 10 mM KCl solution at different pH values. They discovered that the interaction between illite lamellae and the probe tip was attractive when the pH value was 3.0 and repulsive when the pH value ranged within 5.0–10.0. For the interaction between the illite end face and probe tip, there was only a slight attractive force at pH = 3.0; at pH = 5.0, the interaction became a repulsive force; when the pH value ranged from 6.0 to 10.0, the repulsive force increased. The above studies

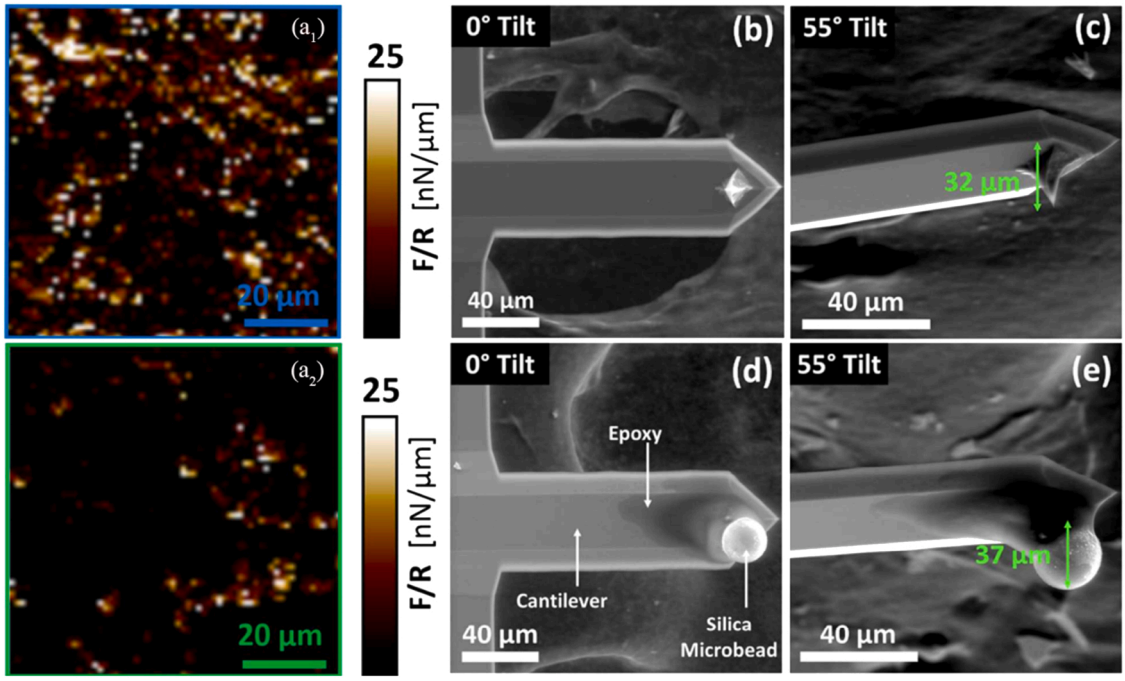

Fig. 4. Adhesion diagrams in the (a_1) dolomite-rich zone and (a_2) natural mineral calcite-rich zone; ESEM images of (b) AFM probe tip and (c) tip length before the wet epoxy resin droplet is attached; ESEM images of (d) AFM probe tip and (e) tip length after the wet epoxy resin droplet is attached (Abed et al., 2018). Adapted with permission from (COMPLETE REFERENCE CITATION). Copyright (2018) American Chemical Society.

show that, in general, the adhesion force between the probe tip and minerals decreases in an alkaline environment and increases in an acidic environment. Therefore, when utilizing the force-distance curve of AFM to investigate the changes in adhesion force on mineral surfaces, great care must be taken to maintain a clean, contamination-free test environment. Otherwise, the wear and contamination of the probe tip will affect the measurement accuracy of the adhesion force.

2.2. Applications of AFM in the research of mineral-aqueous interfaces

The interface refers to the transition zone where two different phases contact each other and transform from one phase to another. Mineral-aqueous interfaces are ubiquitous in nature and affect almost all geochemical processes (Brantley et al., 2008; Gordon and Brown, 2012; Putnis and Ruiz-Agudo, 2013). The AFM has ultra-high atomic scanning resolution, is not limited by the working environment, and has broad applicability. It can conduct research on the mineral-aqueous interfaces at the atomic scale and observe in-situ reaction processes such as dissolution, adsorption, and oxidation at the mineral-aqueous interfaces (Hernández-Muñoz et al., 2020), thereby providing strong support for the research on the mineral-aqueous interfaces.

2.2.1. Dissolution

Mineral dissolution plays a decisive role in the transformation of minerals in the natural environment (He et al., 2019) and is an essential factor affecting the geochemical cycle of chemical elements and the historical changes of the crust. Mineral dissolution usually occurs preferentially at active sites with excessive surface energy, such as defects, dislocations, and grain boundaries, and it is a surface reaction-controlled process. By combining AFM observation with other auxiliary means, the morphology, locations, and dissolution rate of mineral dissolution can be investigated in depth.

The AFM can directly observe the changes of mineral dissolution morphology in different solutions. Bibi et al. (2018) studied the changes in mineral surface topography and dissolution rate on the surface of calcite by using AFM, and a diamond-shaped dissolution morphology was directly observed on the calcite's surface in Na_2CO_3 solution (Fig. 5). The calcite dissolution rate in Pb^{2+}-rich solutions was 50 % slower than in lead-free solutions, and there were few rounded edges at the corners. In contrast, in Pb^{2+}-free solutions, rounded corners and edges were observed, and the dissolution rate at acute angles/edges was faster than that at obtuse angles/edges (Yuan et al., 2019). De Ruiter et al., (2019) observed the in-situ dissolution of quartz in solutions with high pH values and rich Mg^{2+} ions by AFM. They indicated that soft precipitates are formed after the presence of Mg^{2+} ions for 30 min and that the present time and $MgCl_2$ concentration are positively correlated with the number of solid precipitates. Surface defects generated by mineral dissolution can be observed through 3D-AFM images, the observable that enables the imaging of the hydration layers is the amplitude of the tip's oscillation. For example, Songen et al. (2018) used calcite, which is ubiquitous in nature, to conduct defect experiments, and showed the hydration structure at calcite defects by the high-resolution 3D-AFM technique. They demonstrated that the hydration structure at calcite defects is vertically disturbed; even in the fifth hydration layer, the defects of calcite also cause a change in its hydration structure.

In order to investigate the dissolution rate of minerals, most researchers calculate the dissolution rate indirectly by measuring the content of minerals in an aqueous solution; however, it is difficult to describe the specific reaction crystal planes and sites of minerals in macroscopic studies (Qian et al., 2019). Fortunately, the AFM technique can accurately analyze mineral dissolution's location and reaction rate. For example, Dong et al. (2020b) used AFM for the first time to investigate calcite dissolution in seawater, and they found that although calcite dissolves into diamond-shaped morphology in seawater and water with low ionic strength, the volume dissolution rate of calcite in seawater is 2–4 orders of magnitude lower than that in water with low ionic strength. Lange et al. (2021) measured in situ the dissolution rate of alkaline feldspar crystals and demonstrated that the dissolution rate of alkaline feldspar also varies according to different surface textures. They indicated that this phenomenon is related to the mineral geometry and the internal twinned structure in minerals. In order to understand the dissolution rate of a single dolomite crystal, Saldi et al. (2017) estimated the dissolution rate of dolomite single crystal through observing the dissolution rate of carbonate rock surface by AFM, and proposed the mechanisms of surface reaction distribution and reaction rate control. The AFM technique can observe the real time changes of mineral dissolution morphology and estimate the dissolution rate of

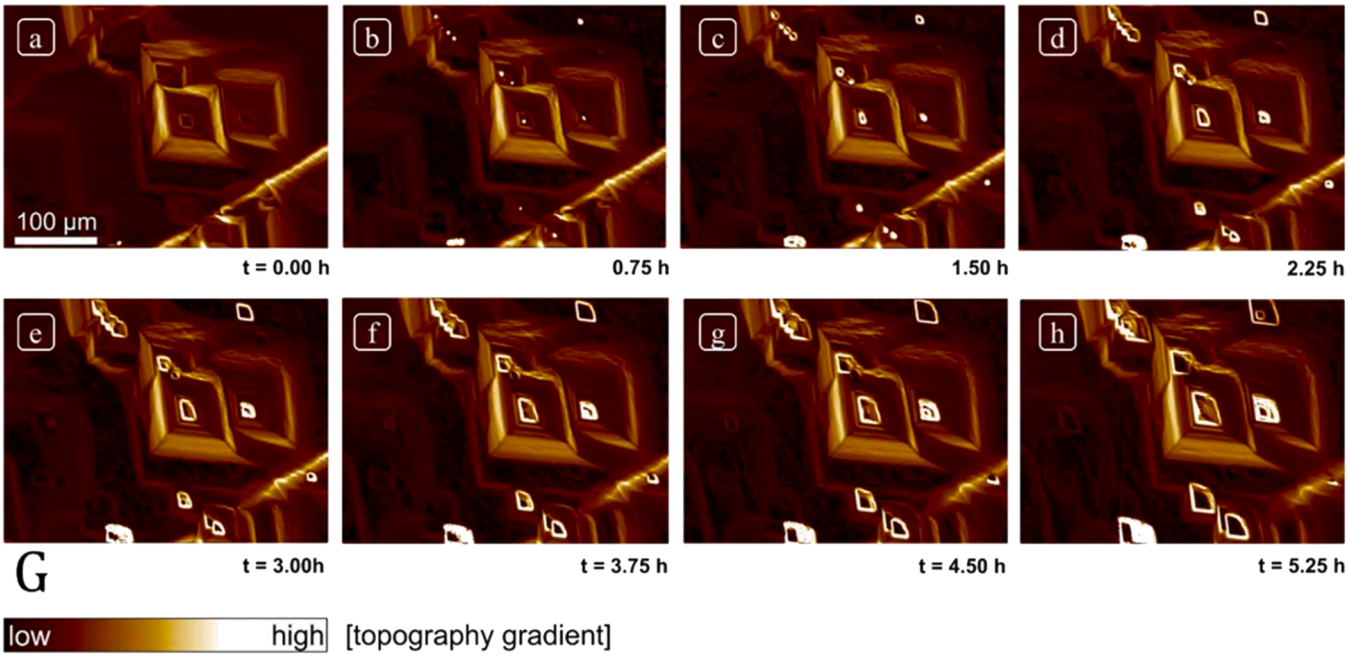

Fig. 5. Morphological images of the dissolution process of calcite (0.75–5.25 h) (Bibi et al., 2018). Copyright (2018), with permission from MDPI.

minerals, which greatly improves people's understanding on mineral dissolution.

2.2.2. Adsorption

The adsorption capacity of minerals for molecules, ions, or other particles in the surrounding environmental media has an important influence on the diagenesis, mineralization, and environmental effects of related elements. Previous studies have shown that many factors, including mineral structure, mineral morphology, and electron-hole pairs, can affect the adsorption capacity of minerals. For example, Songen et al. (2020) revealed the transverse and longitudinal solvation structures of the calcite-ethanol interface and magnesite-ethanol interface by combing 3D-AFM and MD simulations and discovered that the transverse ordered solvation layers of magnesite are similar to those of calcite. Di Iorio et al. (2018) studied arsenate adsorption on hematite, and they discovered that the changes in the morphology of hematite will change its adsorption capacity for nitrate. This is because the hematite lattice has different atomic arrangement periodicity and degrees of density in different directions, which can produce various physical and chemical properties of crystals in different directions. In addition, the electron-hole pairs generated by mineral anisotropy at mineral defects and edges also affect the adsorption capacity of minerals. Yuan et al. (2020) observed through AFM images that the S electron-hole pairs generated at the edges of MoS_2 had a strong affinity for Pb^{2+} particles and deduced the adsorption mechanism of MoS_2 for Pb^{2+} ions. On this basis, they used heat treatment to generate a large number of S electron-hole pairs at the edges of MoS_2, which enhanced the adsorption capacity of MoS^2 for Pb^{2+} ions. Dong et al. (2021) also confirmed the citric acid's strong adsorption and dissolution behaviors on fluorite surfaces through AFM in-situ reaction.

The adsorption properties of minerals will affect their flotation performance. Previous studies examined the adsorption mechanism of rutile surfaces with styrene phosphoric acid (SPA) and Pb^{2+} ionic hydroxyl compounds. They indicated that SPA shows single- and double-layer adsorption on the surface of Pb^{2+} activated rutile surface (the activation of rutile referred to soaking rutile in Pb^{2+} solution for 10 min and then putting it into SPA solution for 10 min) in the form of multimolecular association. In contrast, no adsorption occurs on the surface of the unactivated rutile (the rutile was only put in Pb^{2+} solution or SPA solution for 10 min). These findings help understand the activation process of metal ions on mineral surfaces and enhance the activation effect of rutile flotation (Xiao et al., 2018). The flotation capacity of minerals can be improved by changing the surface properties of minerals to make the adsorption of the flotation agent easier. For example, sodium oleate (NaOL) must be added to the scheelite flotation process. Through AFM technology, it has been observed that adding Pb^{2+} can increase the active sites on the surface of scheelite, which can increase the adsorption capacity of scheelite to NaOL and thus improve the flotation capacity of scheelite (Dong et al., 2019). In addition, AFM 3D height imaging can also be employed to study the adsorption capacity of minerals. For example, Liu et al. (2021) observed calcite and fluorite adsorption reactions with SPA, respectively, through AFM 3D height images. They reported that the amount of hill-like substances on the surface of calcite is much less than that on the surface of fluorite, i.e., the adsorption amount of SPA on calcite is much less than that on fluorite; their work explained the adsorption capacity of different minerals for SPA. Dong et al. (2020a) observed the adsorption morphology and adsorption height of the sodium polyacrylate (PAAS) inhibitor on the surface of calcite using AFM, and they demonstrated that PAAS exhibits a uniform, dense, and punctiform adsorption morphology on the surface of calcite, with an adsorption height of about 4–5 nm (Fig. 6).

The AFM technology can also be applied to the research of mineral adsorption in the field of ecological environment. For example, Qiu et al. (2018) used X-ray scattering and AFM techniques to explore the aggregation process of ZrO_2 nanoparticles on the dolomite's surface. They indicated that with the increase of ionic strength, the number of charges on the surface of nano-ions decreases, leading to the decrease of electrostatic repulsion on the edges of minerals, thus making ZrO_2 nanoparticles aggregate in the lamellae form on the surface of dolomite. Their findings have significant environmental implications for the migration of nano-pollutants. The 3D-AFM imaging technique can also be utilized to detect the adsorption between cells and minerals directly. Abu Quba et al. (2021) utilized a sharp nitride lever (SNL) probe to image bacterial cells on montmorillonite particles, and the distribution of cells on the surface of montmorillonite was clearly observed. In their study, the role of the probe tip between cells and minerals was entirely played, and the detection of cell-mineral adsorption at the single-cell level was realized. In investigating the ion exchange of clay minerals, AFM can be used to explore the adsorption rules of heavy metals on the surface of clay minerals. For example, Araki et al. (2017) observed the atomic scale changes during the exchange of Mg^{2+} ions with Cs^{+} ions on the montmorillonite's surface using FM-AFM, confirming the number of adsorbed Cs^{+} ions depends on the proportion of Mg^{2+} ions in the octahedral layer of montmorillonite. In view of the adsorption of organic compounds on minerals, Moro et al. (2015) used AFM to measure the adsorption of glycine with punctiform, cloddy, and filamentous structures on the (001) crystal plane of brucite. The AFM observation results showed that glycine can be stably and selectively adsorbed on the surface of the hydrophobic layer of brucite to form a single layer with different patterns. In that case, hydrogen bonding mainly adsorbed glycine molecules on the brucite's surface. In addition, Lan et al. (2020) explored the adsorption behaviors of polycyclic aromatic hydrocarbons (PAH) on quartz surface by AFM. They found that with the increase of temperature, the adsorption rate of PAH on quartz surface rises, but the total adsorption amount is basically unchanged; the total thickness of adsorption layer gradually decreases with the increase of temperature, and the distribution of PAH on mineral surfaces is more uniform. The AFM technique is widely used in the research on the adsorption behaviors of mineral-aqueous interfaces. No matter for the adsorption of heavy metals in water pollution or mineral flotation, AFM technique can be utilized to study the surface properties and morphologic changes of minerals, and in-situ observe the adsorption process and products of

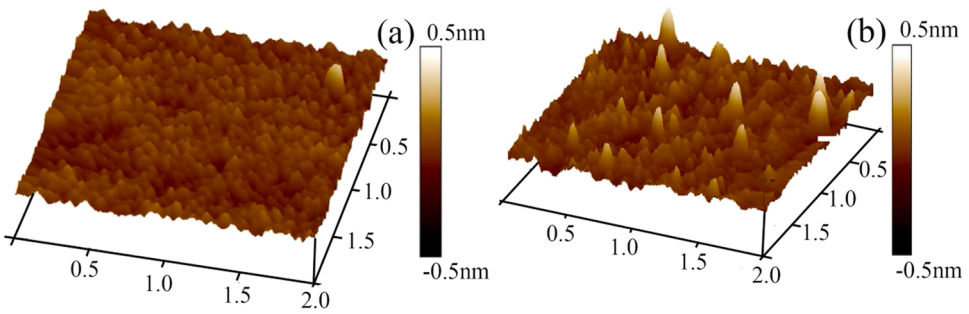

Fig. 6. AFM 3D height images (2 ×2 μm) of the calcite surface (a) before and (b) after the PAAS adsorption reaction (Dong et al., 2020a). Copyright (2020), with permission from Elsevier.

minerals and other substances (heavy metal ions, nanoparticles and organic matter, and others). The AFM technique cannot only improve the utilization rate and extraction rate of minerals, but also play a certain role in the prevention and control of environmental pollution.

2.2.3. Oxidation

Using AFM to study mineral oxidation can directly explore the degree of mineral oxidation and indirectly calculate the rate of mineral oxidation. Among easily oxidized minerals, sulfide minerals can release many pollutants, such as acids and heavy metals, in the oxidation process. Since the release rates of pollutants are controlled by the oxidation kinetics of sulfide minerals, the oxidation of sulfide minerals has been widely concerned (Lu et al., 2002). Jia et al. (2018), for example, studied the oxidation of molybdenite at high temperatures. They indicated, using AFM 3D height images, that the molybdenite's surface was smooth before heat treatment. After heat treatment at 300 ℃ for two hours in the air, no significant changes occurred on the surface. When the temperature was increased to 400 ℃, some equilateral triangle pits appeared on the molybdenite surface. In contrast, etching defects can hardly be observed on the molybdenite surface after low-temperature heat treatment in the air. Their work provides guiding significance for preparing the future adsorbent, catalyst, and other materials from molybdenite. Some researchers also conducted in-depth studies on the oxidation of molybdenite in water (Zhang et al., 2017a; Yi et al., 2019). Through AFM observation, they found that the surface of untreated molybdenite is very smooth. After soaking in pure water for one hour, some needle-like protrusions were observed on the surface of molybdenite due to the oxidation of mineral surfaces (Fig. 7), and the following reactions can occur on the surface of molybdenite in a weakly acidic water environment:

$$MoS_2 + O_2 + H_2O \rightarrow MoO_3 \bullet H_2O + Mo(VI)_xO_y^{a-} + SO_4^{2-} + H^+ \quad (7)$$

where $Mo(VI)_xO_y^{a-}$ is molybdate species containing $Mo(VI)$.

The hydrophobic or hydrophilic products produced by mineral oxidation can affect the physical and chemical properties of mineral surfaces, whereas the flotation performance of minerals is closely related to their surface's physical and chemical properties. Through studying the changes in mineral surface properties during oxidation by AFM, the key factors affecting the flotation process during mineral surface oxidation can be determined, which are very important for optimizing the flotation process. For example, Suyantara et al. (2018) conducted oxidation treatment on chalcopyrite by adding $FeSO_4$ or H_2O_2 aqueous solutions. Based on the AFM images, without adding $FeSO_4$ solution, the surface of chalcopyrite treated with 10 mM H_2O_2 solution was covered with unevenly distributed mountainous features; after treatment with a mixture of 0.1 mM $FeSO_4$ and 10 mM H_2O_2 solutions, the chalcopyrite surface was strongly oxidized and completely covered with "mountainous" substances. The authors considered that the appearance of these "mountainous" substances was attributed to the formation of hydrophilic substances (CuO, $Cu(OH)_2$, FeOOH, and $Fe_2(SO_4)_3$) on the chalcopyrite surface. Their study also demonstrated that the mixture of $FeSO_4$ and H_2O_2 aqueous solution can be utilized to replace NaHS reagents, thus reducing the reagent cost of the copper flotation process. Niu (2019) investigated the oxidation products of pyrite, galena, and chalcopyrite under flotation conditions by AFM, analyzed the influences of such factors as pH value and dissolved oxygen on mineral oxidation and flotation capacity, and established the relationship between surface oxidation and floatability of sulfide minerals, providing a reference for efficient flotation separation technique of sulfide ores. In addition, some researchers also used AFM to analyze the influences of salt ions in seawater on pyrite's oxidation and flotation properties. Pyrite was oxidized in seawater salt solution ($MgCl_2$, NaCl, $CaCl_2$) for 5 min, dried, and then put into sulfonate (PAX) solution for 10 min. After drying, the oxidized pyrite was observed by AFM. It was indicated that pyrite will form interconnected columnar structures after oxidation and that PAX solution was adsorbed on the top and edges of these columns and oxidized into disulfonate. The pyrite oxidized columnar structure significantly improved pyrite flotation capacity (Paredes et al., 2019).

3. Combination of AFM with other instruments

The AFM is an ideal tool that has nano-scale image resolution and mechanical characterization. In addition to those above advances, AFM can also be used with other instruments to provide powerful support for the in-depth study of mineral surface properties. For example, AFM can be combined with Fourier infrared and Raman spectroscopy, which can not only realize real-time observation of sample surface topography but also determine the surface chemical composition of minerals. At present, AFM-Fourier infrared spectroscopy technique and AFM tip enhancement Raman scattering technique have made particular progress in mineral processing and studying the surface properties of mineral materials and have shown certain potential in studying mineral surfaces. Hence, this paper focuses on these two instruments combined with AFM.

3.1. Combination of AFM with Fourier infrared spectroscopy

The resolution of most infrared instruments is limited by optical diffraction. In order to overcome this limitation, scientists have developed AFM-IR, a new device that combines AFM with Fourier infrared spectroscopy. The resolution of AFM-IR is determined by the radius of

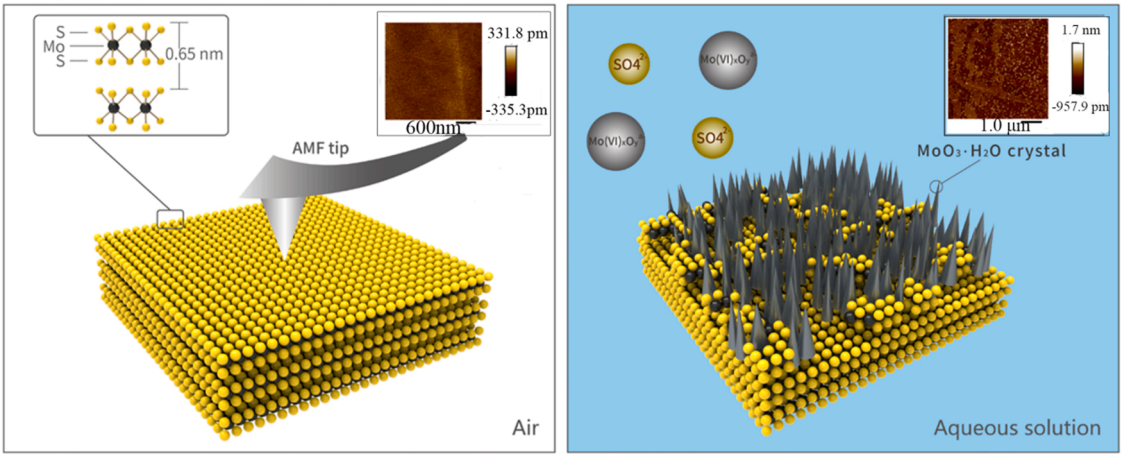

Fig. 7. Schematic diagram of molybdenite oxidation in water: (a) before oxidation, (b) after oxidation (Zhang et al., 2017a). Adapted with permission from (COMPLETE REFERENCE CITATION). Copyright (2017) American Chemical Society.

the AFM tip (in the nanometer range), thus overcoming the limitation of traditional optical diffraction. The AFM tip is used as an infrared detector to measure the mineral surface that absorbs infrared radiation (Zhou et al., 2020). After absorbing infrared light of a specific wavelength, the sample will undergo thermal expansion, which the AFM tip vibration can measure. By measuring the relationship between the cantilever response to infrared absorption and the wavelength, the infrared absorption spectra at the nano-scale can be obtained, and the oscillation spectrum at the AFM tip is proportional to the infrared absorption spectrum (Fig. 8) (Kurouski et al., 2020; Dalby et al., 2018; Dazzi et al., 2012). The contact mode, tapping mode, and peak force mode are generally used in AFM-IR. The metal AFM probe usually has a better effect in achieving local electromagnetic field enhancement at the probe tip (Qian et al., 2018). The AFM-IR technique can improve the spatial resolution of infrared spectra. The operation of AFM-IR is simple. It has low requirements for sample preparation and requires no modeling or data post-processing in subsequent data processing (Mathurin et al., 2022). However, the infrared absorption spectra of water phases are so strong that it is difficult for the probe tip-enhanced infrared spectroscopy to work in the water medium (Xing et al., 2018). On the other hand, the AFM-IR analysis can be affected by the samples' geometric shape. For example, the local shadow generated from the sample thickness, flatness, and adhesion force to the substrate can cause errors in the AFM-IR data analysis (Gr, 2021).

The AFM-IR can cover the infrared spectra of most silicates, so it is widely used in minerals and materials research (Wang et al., 2021a). Yang et al. (2017) measured the chemical and mechanical inhomogeneity of nano-scale solid organic matter (OM) in shale by optical mapping and point spectroscopy, which had a spatial resolution of one or more orders of magnitude smaller than that of traditional infrared microscopes. Jubb et al. (2019) used AFM-IR with a spatial resolution of 50 nm to evaluate the relationship between the petroleum molecules and the surface of carbonate rocks. They found that petroleum molecules are distributed from the organic-rich "source stratum" to the carbonate "reservoir stratum" beyond 150 μm. The organic matter immediately began to change after it was discharged from the organic "source stratum"; the carbonyl groups were lost, and the length of alkyl chains decreased. The authors suggested that this phenomenon was due to the interaction of granular mineral surfaces and that the fractionation effect was enhanced by increasing the distance from the organic-rich "source stratum" to the carbonate "reservoir stratum". The AFM-IR combines the existing infrared spectroscopy technique with the AFM technique, which can obtain infrared absorption spectra and absorption images with a spatial resolution of 50–100 nm. This is improves the spatial resolution of traditional infrared spectra and retain the advantages of infrared spectrum measurement on the sample non-destructive. However, AFM-IR still has some shortcomings. For example, it cannot be applied in liquid environment measurement, and its application field is not comprehensive enough.

3.2. Combination of AFM with Raman scattering spectroscopy

Scanning probe microscopy (SPM) techniques include scanning tunneling microscopy (STM), scanning shear-force microscopy (SFM), and AFM. By combining SPM with the Raman technique, a novel surface analysis technique at the nano-scale, namely tip-enhanced Raman scattering (TERS) (Cao and Sun, 2022; Shao and Zenobi, 2019; Jiang et al., 2016), can be developed. The TERS technique has attracted more and more attention due to its simple operation, wide application range, and high spatial resolution and sensitivity (Kumar et al., 2019). The basic principles of TERS are as follows. By controlling the contact between the metal or metalized probe tip and the sample, a localized solid electromagnetic field can be generated between the probe and the sample under the surface plasmon resonance effect when an incident light with an appropriate wavelength irradiates on the probe tip. In this case, Raman signals of the sample under the probe tip will be enhanced, and the physicochemical information of the sample can be obtained utilizing non-metric spatial resolution. Fig. 9 indicates that a laser beam (λ_1) focuses on the sample's surface, and a sharp metal tip is placed where the laser is focused. The enhanced field of the tip interacts locally with the sample's surface to excite the spectral response (λ_2), which is collected by the same objective lens and directed to the detector (Langeluddecke et al., 2015; Xiao and Schultz, 2018). The probe tip, usually Au or Ag tip, is an essential part of TERS. It determines the intensity of TERS signals and affects samples' spatial resolution and imaging quality. Hence, the stability, resolution, and quality of the TERS tip are crucial (Huang et al., 2018).

As one of the tools to identify chemical substances, TERS solves the deficiency that AFM-IR cannot be applied in liquid environment measurement. It can obtain the properties of substances generated at the mineral-aqueous interfaces and break through the spatial resolution of the optical diffraction limit. Under the directional imaging mode of AFM, the complementarity of these two methods by confocal Raman spectroscopy can achieve mechanical and chemical characterization with high sensitivity and sub-nano lateral resolution (Casdorff et al., 2018). Nowadays, the TERS technique has become an advanced tool. It can image the morphology and roughness of samples with sub-nanometer resolution and the chemical composition and functional groups by Raman spectroscopy. Therefore, TERS has great application prospects in characterizing one- and two-dimensional nanomaterials, semiconductors, organic compounds, and polymers (Kurouski, 2017).

In investigating the mineral surface properties, TERS is involved the surface properties of cassiterite, magnesite, chalcopyrite, and other minerals. For example, Babel and Rudolph (Babel and Rudolph, 2019) utilized the colloid probe AFM Raman (CP-AFM Raman) for the first time to measure the wettability of cassiterite and obtained the Raman spectra of cassiterite with a spatial resolution of 1 μm. Borromeo et al. (2018) used TERS to study the high-resolution topographic maps and

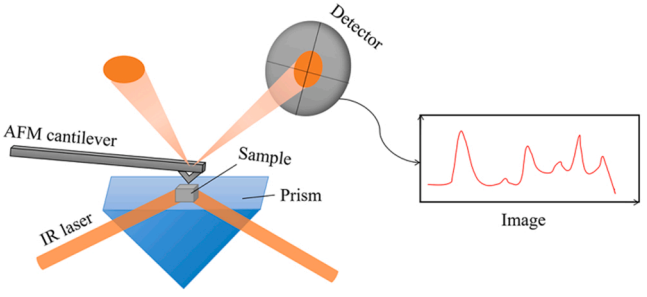

Fig. 8. Schematic diagram of AFM-IR (Dazzi and Prater, 2017). Adapted with permission from (COMPLETE REFERENCE CITATION). Copyright (2017) American Chemical Society.

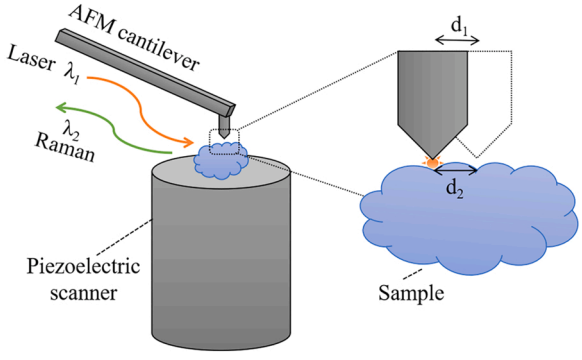

Fig. 9. Schematic diagram of TERS (Xiao and Schultz, 2018). Adapted with permission from (COMPLETE REFERENCE CITATION). Copyright (2018) American Chemical Society.

mineralogical diagrams of chalk cores in a mixed solution of magnesium chloride (0.219 M) and calcium chloride (0.13 M) under specific temperature, pressure, and pH conditions (i.e., hydrocarbon reservoir conditions in the chalk of the Norwegian continental shelf). They indicated that the secondary growth of magnesite was not widespread on the 718th day of the experiment, but an almost pure magnesite composition was detected on the 1072nd day. Qian et al. (2020) studied the reactivity of the (112) surface of chalcopyrite under industry-related leaching conditions by TERS. They demonstrated no leaching of S element from chalcopyrite in Fe^{3+} and Fe^{2+} solutions within 42 days, indicating that the (112) surface of chalcopyrite is relatively inert. The TERS technique can reveal the chemical information of minerals and observe and analyze the changes in minerals and the composition of grown materials at the nano-scale. As gold probes are soft, they are easily damaged during use. Silver probes have a high enhancement factor but oxidizes rapidly in air, which makes the reproducibility of the enhanced Raman signal difficult, so protection of the probes is also extremely important (Festy et al., 2004; Hu et al., 2003; Krug et al., 2002; Richards et al., 2003). In the next few years, the complementary characterization of chemical components based on spectroscopy and the development of force sensors for simultaneous measurement of force and displacement will be hot topics, which can provide new ideas for understanding the mineral surface properties.

To sum up, both AFM-IR and TERS can be employed to examine mineral surface properties, and both have strengths and weaknesses. When measuring mineral surface properties, the test instrument should be selected according to specific demands and conditions. Table 1 summarizes the strengths and weaknesses and the application scopes of AFM-IR and TERS.

4. Summary and prospects

This study reviews the applications of AFM and its combined techniques in mineralogical research. First, AFM can be applied in 2D and 3D imaging of mineral surfaces. Through the imaging of minerals by AFM technique, the changes of mineral surfaces, such as the dissolution, adsorption, and oxidation of minerals, can be in-situ observed, and the interaction mechanism and behaviors of mineral-aqueous interfaces can be intuitively understood. Second, the AFM technique can be used for the mechanical measurement of mineral surfaces. The force interactions between the AFM probe and minerals can be explored by measuring the adhesion force between minerals and other substances (minerals, flotation agents, and others). Third, AFM can be combined with other instruments. The extremely high spatial resolution of AFM, coupled with the chemical recognition of the Fourier infrared spectrum and Raman spectrum, can realize the dual research of physical and chemical properties of mineral surfaces.

Table 1
Strengths, weaknesses, and application scopes of AFM-IR and TERS.

	Strengths	Weaknesses	Application scopes	Literature
AFM-IR	Simple operation, low requirements for sample preparation, high reliability, simple data processing; Traditional optical diffraction limitations can be overcome	Samples cannot be tested in a liquid environment	The relationship between petroleum molecules and minerals; Polymer composites	(Wang et al., 2021a; Yang et al., 2017; Jubb et al., 2019)
TERS	Samples can be tested in a liquid environment with high resolution (up to 0.5 nm); Morphology and spectral information of samples can be obtained simultaneously; High detection sensitivity and low requirements for sample preparation	Complex operation; tough preparation process of tip; Low reproducibility of Raman signal enhancement	Nanomaterials, semiconductors, organic compounds, and polymers	(Babel and Rudolph, 2019; Borromeo et al., 2018; Qian et al., 2020)

In recent years, AFM has been applied more and more widely in mineralogy research, but there are still some deficiencies in AFM. In order to solve these problems, this provides corresponding suggestions. (1) AFM tip is vulnerable to contamination in the scanning process, especially in the multi-dimensional and multi-component test environment. If there is an intelligent AFM probe with automatic cleaning and high environmental adaptability in the future, the wear and loss of the AFM probe will be significantly reduced. (2) The sensitivity of the AFM probe determines the success or failure of the nano-scale technological operation. It is necessary to improve the sensitivity of AFM during the operations of nano-etching, nanomanipulation, and monomolecular stretching techniques. By changing the tip of the probe or adjusting the length and elasticity of the cantilever, it can be possible to improve the sensitivity of the AFM probe. (3) In the research process of mineral-aqueous interfaces, the oxidation of minerals, for example, the pyrite that has a very fast oxidation rate, can be completed in the scanning process of the AFM tip. Hence, the test procedure should be as simple as possible to improve the AFM imaging speed and obtain more accurate experimental data. (4) As AFM does not have the capability to test the composition of samples, it is possible to combine AFM with an instrument for elemental analysis (e.g. XRD, XPS and EDS) to enhance the ability to analysis structural changes in samples and to detect the composition and morphology of samples at the same time, providing some assistance in the exploitation of minerals. (5) Developing environmental cells in AFM with a wider range of temperatures, pressures and more complex chemical conditions will provide new opportunities to study more complex reactions in mineral-aqueous interfaces (e.g. studies of mineral transformations deep in the Earth). More complex environmental cells in AFM for surface study are important to simulate and monitor the dynamic process so that it is comparable to real conditions.

Although AFM technology has been used in many fields and impressive progress has been made, the technology of AFM is not perfect at present. If AFM can further optimize the structure, such as improving the probe tip size, developing intelligent probes or even multi-probe systems, increasing the scanning speed and selecting better mechanical properties of probe materials, will increase the range of uses for the AFM. In addition, the AFM could be expanded in terms of function, such as combining with other inspection techniques, developing more scanning modes, further development towards improving spatial and temporal resolution, I believe AFM can be better used for us. It will be possible to study mineralogy more extensively, conveniently and comprehensively through the continuous improvement and updating of atomic force microscopy techniques. This will provide more in-depth investigations of the geochemical cycle, provide more guiding advices on ecological and environmental issues and geological research, and have a profound impact on future mineralogy-related research and practice.

Declaration of Competing Interest

The authors declare that they have no known competing financial interests or personal relationships that could have appeared to influence

the work reported in this paper.

Data availability

Data will be made available on request.

Acknowledgement

Y.H. Fu gratefully acknowledges the support from Guizhou Provincial Science and Technology Foundation (Qian Sci. Co. ZK [2021] No.198), and the National Natural Science Foundation of China (42162006).

References

Abed, J., Aubry, C., Zaidani, M., El Hadri, N., Devarapalli, R., Jouiad, M., 2018. Determination of dead-oil wetting and adhesive forces on carbonate rocks using colloidal-probe atomic force microscopy. Energy Fuels 32, 9182–9190. https://doi.org/10.1021/acs.energyfuels.8b01941.

Abouelatta, O.B., Mádl, J., 2001. Surface roughness prediction based on cutting parameters and tool vibrations in turning operations. J. Mater. Process. Technol. 118 (1–3), 269–277. https://doi.org/10.1016/S0924-0136(01)00959-1.

Abu Quba, A.A., Schaumann, G.E., Karagulyan, M., Diehl, D., 2021. Quality control of direct cell-mineral adhesion measurements in air and liquid using inverse AFM imaging. RSC Adv. 11, 5384–5392. https://doi.org/10.1039/d1ra00110h.

Al Maskari, N.S., Xie, Q., Saeedi, A., 2019. Role of basal-charged clays in low salinity effect in sandstone reservoirs: adhesion force on muscovite using atomic force microscope. Energy Fuels 33, 756–764. https://doi.org/10.1021/acs.energyfuels.8b03452.

Alnoush, W., Sayed, A., Solling, T.I., Alyafei, N., 2021. Impact of calcite surface roughness in wettability assessment: interferometry and atomic force microscopy analysis. J. Pet. Sci. Eng. 203, 108679 https://doi.org/10.1016/j.petrol.2021.108679.

Altiner, M., 2019. Effect of base types on the properties of MgO particles obtained from dolomite ore. Min. Metall. Explor. 36, 1013–1020. https://doi.org/10.1007/s42461-019-00122-7.

Alvim, R.D.S., Miranda, C.R., 2016. Noncontact AFM first-principles simulations of functionalized silicon tips on the montmorillonite (001) surface. J. Phys. Chem. C 120, 13503–13513. https://doi.org/10.1021/acs.jpcc.6b01319.

Araki, Y., Satoh, H., Okumura, M., Onishi, H., 2017. Localization of cesium on montmorillonite surface investigated by frequency modulation atomic force microscopy. Surf. Sci. 665, 32–36. https://doi.org/10.1016/j.susc.2017.08.004.

Azghdi, S.M.S., Barani, K., 2018. Effect of microwave treatment on the surface properties of chalcopyrite. Miner. Metall. Process. 35, 141–147. https://doi.org/10.19150/mmp.8463.

Babel, B., Rudolph, M., 2019. Co-localized (colloidal probe) atomic force microscopy/Raman spectroscopy measurements for hydrophobicity characterization. Miner. Eng. 141, 105838 https://doi.org/10.1016/j.mineng.2019.105838.

Bai, T.A., Yang, F., Wang, H., Zheng, H., 2022W. Adhesion forces of shale oil droplet on mica surface with different roughness: an experimental investigation using atomic force microscopy. Energies 15, 6460. https://doi.org/10.3390/en15176460.

Bian, K., Gerber, C., Heinrich, A.J., Müller, D.J., Scheuring, S., Jiang, Y., 2021. Scanning probe microscopy. Nat. Rev. Methods Prim. 1. https://doi.org/10.1038/s43586-021-00033-2.

Bibi, I., Arvidson, R., Fischer, C., Lüttge, A., 2018. Temporal evolution of calcite surface dissolution kinetics. Minerals 8, 256. https://doi.org/10.3390/min8060256.

Binnig, G., Rohrer, H., 1982. Scanning tunneling microscope. Surf. Sci. 126, 236–244.

Binnig, G., Quate, C.F., Gerber, C., 1986. Atomic force microscope. Phys. Rev. Lett. 56, 930–933. https://doi.org/10.1103/PhysRevLett.56.930.

Borromeo, L., Toccafondi, C., Minde, M.W., Zimmermann, U., Andò, S., Madland, M.V., et al., 2018. Application of tip-enhanced Raman spectroscopy for the nanoscale characterization of flooded chalk. J. Appl. Phys. 124, 173101 https://doi.org/10.1063/1.5049823.

Brantley, S.L., Kubicki, J.D., White, A.F., 2008. Kinetics of Water-Rock Interaction. Springer, New York, NY, pp. 73–101. https://doi.org/10.1007/978-0-387-73563-4.

Cao, Y., Sun, M., 2022. Tip-enhanced Raman spectroscopy. Rev. Phys. 8, 100067 https://doi.org/10.1016/j.revip.2022.100067.

Casdorff, K., Kläusler, O., Gabriel, J., Amen, C., Lehringer, C., Burgert, I., et al., 2018. About the influence of a water-based priming system on the interactions between wood and one-component polyurethane adhesive studied by atomic force microscopy and confocal Raman spectroscopy imaging. Int. J. Adhes. Adhes. 80, 52–59. https://doi.org/10.1016/j.ijadhadh.2017.10.001.

Chang, W.R., Kim, I.J., Manning, D.P., Bunterngchit, Y., 2001. The role of surface roughness in the measurement of slipperiness. Ergonomics 44, 1200–1216. https://doi.org/10.1080/00140130110085565.

Chen, Y., Huang, W., 2004. Numerical simulation of the geometrical factors affecting surface roughness measurements by AFM. Meas. Sci. Technol. 15, 2005–2010. https://doi.org/10.1088/0957-0233/15/10/010.

Couto, M.S., van Enckevort, W.J.P., Seal, M., 2006. Diamond polishing mechanisms: an investigation by scanning tunnelling microscopy. Philos. Mag. B. 69, 621–641. https://doi.org/10.1080/01418639408240133.

Dalby, K.N., Berger, J.A., Brand, H.E.A., Cairney, J.M., Eder, K., Eggins, S.M., et al., 2018. Analytical techniques for probing small-scale layers that preserve information on gas–solid interactions. Rev. Mineral. Geochem. 84, 103–175. https://doi.org/10.2138/rmg.2018.84.4.

Dazzi, A., Prater, C.B., 2017. AFM-IR: technology and applications in nanoscale infrared spectroscopy and chemical imaging. Chem. Rev. 117, 5146–5173. https://doi.org/10.1021/acs.chemrev.6b00448.

Dazzi, A., Prater, C.B., Hu, Q., Chase, D.B., Rabolt, J.F., Marcott, C., 2012. AFM–IR: combining atomic force microscopy and infrared spectroscopy for nanoscale chemical characterization. Appl. Spectrosc. 66, 1365–1384.

De Ruiter, L., Putnis, C.V., Hövelmann, J., King, H.E., Austrheim, H., 2019. Direct observations of the coupling between quartz dissolution and Mg-silicate formation. Earth Space Chem 27.

Deng, X., Tang, Y., Zhou, Y., Yang, Y., S. H, 2018. High-resolution surface topography measurement based on frequency-domain analysis in white light interferometry. Chin. Laser Press 45, 112–118.

Di Iorio, E., Cho, H.G., Liu, Y., Cheng, Z., Angelico, R., Colombo, C., 2018. Arsenate retention mechanisms on hematite with different morphologies evaluated using AFM, TEM measurements and vibrational spectroscopy. Geochim. Cosmochim. Acta 237, 155–170. https://doi.org/10.1016/j.gca.2018.06.027.

Ding, H., Mettu, S., Rahman, S., 2020. Probing the effects of Ca^{2+}, Mg^{2+}, and SO_4^{2-} on calcite–oil interactions by "Soft Tip" atomic force microscopy (AFM). Ind. Eng. Chem. Res. 59, 13069–13078. https://doi.org/10.1021/acs.iecr.0c01665.

Dobryden, I., Potapova, E., Holmgren, A., Weber, H., Hedlund, J., Almqvist, N., 2014. Force interactions between magnetite, silica, and bentonite studied with atomic force microscopy. Phys. Chem. Miner. 42, 319–326. https://doi.org/10.1007/s00269-014-0722-9.

Dong, L., Wei, Q., Qin, W., Jiao, F., 2020b. Selective adsorption of sodium polyacrylate on calcite surface: implications for flotation separation of apatite from calcite. Sep. Purif. Technol. 241, 116415 https://doi.org/10.1016/j.seppur.2019.116415.

Dong, L., Jiao, F., Qin, W., Wei, Q., 2021. New insights into the depressive mechanism of citric acid in the selective flotation of scheelite from fluorite. Miner. Eng. 171, 107117 https://doi.org/10.1016/j.mineng.2021.107117.

Dong, L., Jiao, F., Qin, W., Zhu, H., Jia, W., 2019. Activation effect of lead ions on scheelite flotation: adsorption mechanism, AFM imaging and adsorption model. Sep. Purif. Technol. 209, 955–963. https://doi.org/10.1016/j.seppur.2018.09.051.

Dong, S., Berelson, W.M., Adkins, J.F., Rollins, N.E., Naviaux, J.D., Pirbadian, S., et al., 2020a. An atomic force microscopy study of calcite dissolution in seawater. Geochim. Cosmochim. Acta 283, 40–53. https://doi.org/10.1016/j.gca.2020.05.031.

El-Nagar, D.A., Abdel-Halim, K.Y., 2021. Remediation of heavy metals in contaminated soil by using nano-bentonite, nano-hydroxyapatite, and nano-composite. Land Degrad. Dev. 32, 4562–4573. https://doi.org/10.1002/ldr.4052.

Fava, M., Frascino, A.V., Balducci, I., Ramos, C.J., 2018W. Comparative analysis of different prophylatic methods on primary teeth enamel roughness. Braz. Dent. Sci. 21, 335–340. https://doi.org/10.14295/bds.2018.v21i3.1567.

Feng, B., Liu, H., Li, Y., Liu, X., Tian, R., Li, R., et al., 2020. AFM measurements of Hofmeister effects on clay mineral particle interaction forces. Appl. Clay Sci. 186, 105443 https://doi.org/10.1016/j.clay.2020.105443.

Festy, F., Demming, A., Richards, D., 2004. Resonant excitation of tip plasmons for tip-enhanced Raman SNOM. Ultramicroscopy 100, 437–441. https://doi.org/10.1016/j.ultramic.2003.11.019.

Fukuma, T., Garcia, R., 2018. Atomic- and molecular-resolution mapping of solid-liquid interfaces by 3D atomic force microscopy. ACS Nano 12, 11785–11797. https://doi.org/10.1021/acsnano.8b07216.

Gan, Y., 2009. Atomic and subnanometer resolution in ambient conditions by atomic force microscopy. Surf. Sci. Rep. 64, 99–121. https://doi.org/10.1016/j.surfrep.2008.12.001.

Garcia, R.A., Avendaño, C.M., Pal, M., Delgado, F.P., Mathews, N.R., 2016. Antimony sulfide (Sb2S3) thin films by pulse electrodeposition: effect of thermal treatment on structural, optical and electrical properties. Mater. Sci. Semicond. Process. 44, 91–100. https://doi.org/10.1016/j.mssp.2015.12.018.

Gordon, E., Brown, G.C., 2012. Mineral-aqueous solution interfaces and their impact on the environment. Geochem. Perspect. (4–5), 483–742.

Gr, B., 2021. Cometary Dust and Origin of Matter in the Protoplanetary Disk. Université Paris-Saclay.

Gross, L., Schuler, B., Pavlicek, N., Fatayer, S., Majzik, Z., Moll, N., et al., 2018. Atomic force microscopy for molecular structure elucidation. Angew. Chem. Int Ed. Engl. 57, 3888–3908. https://doi.org/10.1002/anie.201703509.

Hansma, P.K., Cleveland, J.P., Radmacher, M., Walters, D.A., Hillner, P.E., Bezanilla, M., et al., 1994. Tapping mode atomic force microscopy in liquids. Appl. Phys. Lett. 64, 1738–1740. https://doi.org/10.1063/1.111795.

He, H., Cao, J., Duan, N., 2019. Defects and their behaviors in mineral dissolution under water environment: a review. Sci. Total Environ. 651, 2208–2217. https://doi.org/10.1016/j.scitotenv.2018.10.151.

He, H., Zhu, J., Chen, M., Tao, Q., Tan D, X.L., 2020. Progresses in researches on mineral structure and mineral physics (2011-2020). Bull. MIneral. Petrol. Geochem. 39, 697–713+682. https://doi.org/10.19658/j.issn.1007-2802.2020.39.058.

Hernández-Muñoz, J., Uhlig, M.R., Benaglia, S., Chacón, E., Tarazona, P., Garcia, R., 2020. Subnanometer interfacial forces in three-dimensional atomic force microscopy: water and octane near a mica surface. J. Phys. Chem. C 124, 26296–26303. https://doi.org/10.1021/acs.jpcc.0c08092.

Hirsekorn, S., Rabe, U., Arnold, W., 1997. Theoretical description of the transfer of vibrations from a sample to the cantilever of an atomic force microscope. Nanotechnology 8 (2), 57–63. https://doi.org/10.1088/0957-4484/8/2/003.

Hong, H., Zhang, H., Zhang, S., 2020. Effect of multi-dimensional nanomaterials on the aging behavior of asphalt by atomic force microscope. Constr. Build. Mater. 260, 120389 https://doi.org/10.1016/j.conbuildmat.2020.120389.
Hu, D., Micic, M., Klymyshyn, N., Suh, Y.D., Lu, H.P., 2003. Correlated topographic and spectroscopic imaging beyond diffraction limit by atomic force microscopy metallic tip-enhanced near-field fluorescence lifetime microscopy. Rev. Sci. Instrum. 74, 3347–3355. https://doi.org/10.1063/1.1581359.
Huang, T.X., Li, C.W., Yang, L.K., Zhu, J.F., Yao, X., Liu, C., et al., 2018. Rational fabrication of silver-coated AFM TERS tips with a high enhancement and long lifetime. Nanoscale 10, 4398–4405. https://doi.org/10.1039/c7nr08186c.
Ismail, R.A., Hamoudi, W.K., Shakir, Z.S., 2020. Modifications of Hydroxyapatite properties by nanosecond Nd: YAG laser pulses. Lasers Manuf. Mater. Process. 7, 305–316. https://doi.org/10.1007/s40516-020-00123-1.
Jia, F., Liu, C., Yang, B., Song, S., 2018. Microscale control of edge defect and oxidation on molybdenum disulfide through thermal treatment in air and nitrogen atmospheres. Appl. Surf. Sci. 462, 471–479. https://doi.org/10.1016/j.apsusc.2018.08.166.
Jiang, N., Kurouski, D., Pozzi, E.A., Chiang, N., Hersam, M.C., Van Duyne, R.P., 2016. Tip-enhanced Raman spectroscopy: from concepts to practical applications. Chem. Phys. Lett. 659, 16–24. https://doi.org/10.1016/j.cplett.2016.06.035.
Jin, Q., Li, G., Wang, H., Liu, J., Zhang, J., 2015. Application of the nanoindentation technique in material machanics test. Surf. Technol. 44, 127–136. https://doi.org/10.16490/j.cnki.issn.1001-3660.2015.12.021.
Jubb, A.M., Hackley, P.C., Hatcherian, J.J., Qu, J., Nesheim, T.O., 2019. Nanoscale molecular fractionation of organic matter within unconventional petroleum source beds. Energy Fuels 33, 9759–9766. https://doi.org/10.1021/acs.energyfuels.9b02518.
Jupille, J., 2014. Analysis of mineral surfaces by atomic force microscopy. Rev. Mineral. Geochem. 78, 331–369. https://doi.org/10.2138/rmg.2014.78.8.
Kolchuzhin, V.A., Sheremet, E., Bhattacharya, K., Rodriguez, R.D., Paul, S.D., Mehner, J., et al., 2016. Mechanical properties and applications of custom-built gold AFM cantilevers. Mechatronics 40, 281–286. https://doi.org/10.1016/j.mechatronics.2016.05.015.
Koporulina, E.V., Ryazantseva, M.V., Chanturiya, E.L., Zhuravleva, E.S., 2018. Butyl-xanthate adsorption on the surface of sulfide minerals under conditions of their preliminary treatment with water electrolysis products according to atomic-force microscopy and infrared fourier spectroscopy data. J. Surf. Investig. X-ray Synchrotron Neutron Tech. 12, 877–886. https://doi.org/10.1134/s1027451018050075.
Krug, J.T., Sánchez, E.J., Xie, X.S., 2002. Design of near-field optical probes with optimal field enhancement by finite difference time domain electromagnetic simulation. J. Chem. Phys. 116, 10895–10901. https://doi.org/10.1063/1.1479723.
Kumar, N., Weckhuysen, B.M., Wain, A.J., Pollard, A.J., 2019. Nanoscale chemical imaging using tip-enhanced Raman spectroscopy. Nat. Protoc. 14, 1169–1193. https://doi.org/10.1038/s41596-019-0132-z.
Kurouski, D., 2017. Advances of tip-enhanced Raman spectroscopy (TERS) in electrochemistry, biochemistry, and surface science. Vib. Spectrosc. 91, 3–15. https://doi.org/10.1016/j.vibspec.2016.06.004.
Kurouski, D., Dazzi, A., Zenobi, R., Centrone, A., 2020. Infrared and Raman chemical imaging and spectroscopy at the nanoscale. Chem. Soc. Rev. 49, 3315–3347. https://doi.org/10.1039/c8cs00916c.
Lan, T., Liu, J., Zeng, H., Tang, T., 2020. Temperature-induced transition from indirect to direct adsorption of polycyclic aromatic hydrocarbons on quartz: a combined theoretical and experimental study. Ind. Eng. Chem. Res. 59, 18500–18509. https://doi.org/10.1021/acs.iecr.0c02412.
Lange, I., Toro, M., Arvidson, R.S., Kurganskaya, I., Luttge, A., 2021. The role of crystal heterogeneity in alkali feldspar dissolution kinetics. Geochim. Cosmochim. Acta 309, 329–351. https://doi.org/10.1016/j.gca.2021.06.032.
Langeluddecke, L., Singh, P., Deckert, V., 2015. Exploring the nanoscale: fifteen years of tip-enhanced Raman spectroscopy. Appl. Spectrosc. 69, 1357–1371. https://doi.org/10.1366/15-08014.
Li, Z., Rao, F., Corona-Arroyo, M.A., Bedolla-Jacuinde, A., Song, S., 2019. Comminution effect on surface roughness and flotation behavior of malachite particles. Miner. Eng. 132, 1–7. https://doi.org/10.1016/j.mineng.2018.11.056.
Liu, J., Xie, R., Zhu, Y., Li, Y., Liu, C., 2021. Flotation behavior and mechanism of styrene phosphonic acid as collector on the flotation separation of fluorite from calcite. J. Mol. Liq. 326, 115261 https://doi.org/10.1016/j.molliq.2020.115261.
Liu, X., 2003. Crystal Structure and Surface Property of Diaspore and Phyllosilicate Minerals (Doctor). Central South University.
Liu, Y., Wang, H., Sun, D., Wang, M., Yao, W., X. Y, 2003. An atomic force microscope and its application. Sci. Technol. Rev. 9–12.
López, J., Reig, M., Gibert, O., Torres, E., Ayora, C., Cortina, J.L., 2018. Application of nanofiltration for acidic waters containing rare earth elements: influence of transition elements, acidity and membrane stability. Desalination 430, 33–44. https://doi.org/10.1016/j.desal.2017.12.033.
Lu, L., Lei, L., Lin, J., Zhang, P., 2002. Study on the physical and reactive nature of mineral surfaces: advances and applications. J. Guilin Univ. Technol. 354–358.
Maskari, N.S.A., Sari, A., Hossain, M.M., Saeedi, A., Xie, Q., 2019. Response of non-polar oil component on low salinity effect in carbonate reservoirs: adhesion force measurement using atomic force microscopy. Energies 13, 77. https://doi.org/10.3390/en13010077.
Mathurin, J., Deniset-Besseau, A., Bazin, D., Dartois, E., Wagner, M., Dazzi, A., 2022. Photothermal AFM-IR spectroscopy and imaging: status, challenges, and trends. Appl. Phys. 131 https://doi.org/10.1063/5.0063902.
Misumi, I., Sugawara, K., Kizu, R., Hirai, A., Gonda, S., 2019. Extension of the range of profile surface roughness measurements using metrological atomic force microscope. Precis. Eng. 56, 321–329. https://doi.org/10.1016/j.precisioneng.2019.01.002.
Moro, D., Ulian, G., Valdre, G., 2015. Single molecule investigation of glycine chlorite interaction by cross correlated scanning probe microscopy and quantum mechanics simulations. Langmuir 31, 4453–4463. https://doi.org/10.1021/acs.langmuir.5b00161.
Muller, V.M., Yushchenko, V.S., Derjaguin, B.V., 1980. On the influence of molecular forces on the deformation of an elastic sphere and its sticking to a rigid plane. Colloid Interface Sci. 77 (1), 91–101.
Muneer, R., Hashmet, M.R., Pourafshary, P., 2020. Fine migration control in sandstones: surface force analysis and application of DLVO theory. ACS Omega 5, 31624–31639. https://doi.org/10.1021/acsomega.0c03943.
Niu, X., 2019. Correlation of Surface Oxidation of Galena, Chalcopyrite and Pyrite with Their Floatability (Doctor). University of Chinese Academy of Sciences,.
Paredes, Á., Acuña, S.M., Toledo, P.G., 2019. AFM study of pyrite oxidation and xanthate adsorption in the presence of seawater salts. Metals 9, 1177. https://doi.org/10.3390/met9111177.
Paulo, Á.S., García, R., 2002. Unifying theory of tapping-mode atomic-force microscopy. Phys. Rev. B 66. https://doi.org/10.1103/PhysRevB.66.041406.
Perec, A., Pude, F., Kaufeld, M., Wegener, K., 2017. Obtaining the selected surface roughness by means of mathematical model based parameter optimization in abrasive waterjet cutting. Stroj. Vestn. J. Mech. Eng. 63, 606–613. https://doi.org/10.5545/sv-jme.2017.4463.
Putnis, C.V., Ruiz-Agudo, E., 2013. The mineral-water interface: where minerals react with the environment. Elements 9, 177–182. https://doi.org/10.2113/gselements.9.3.177.
Qian, G., Gibson, C.T., Harmer-Bassell, S., Pring, A., 2020. Atomic force microscopy and raman microspectroscopy investigations of the leaching of chalcopyrite (112) surface. Minerals 10, 485. https://doi.org/10.3390/min10060485.
Qian, G., Fan, R., Short, M.D., Schumann, R.C., Li, J., Li, Y., et al., 2019. Evaluation of the rate of dissolution of secondary sulfate minerals for effective acid and metalliferous drainage mitigation. Chem. Geol. 504, 14–27. https://doi.org/10.1016/j.chemgeo.2018.12.003.
Qian, W., Sun, S., Song, J., Nguyen, C., Ducharme, S., Turner, J.A., 2018. Focused electron-beam-induced deposition for fabrication of highly durable and sensitive metallic AFM-IR probes. Nanotechnology 29, 335702. https://doi.org/10.1088/1361-6528/aac73c.
Qiu, C., Eng, P.J., Hennig, C., Schmidt, M., 2018. Formation and aggregation of ZrO2 nanoparticles on muscovite (001). J. Phys. Chem. C 122, 3865–3874. https://doi.org/10.1021/acs.jpcc.7b10101.
Qudoos, A., Kim, H.G., Ryou, J.S., 2018. Influence of the surface roughness of crushed natural aggregates on the microhardness of the interfacial transition zone of concrete with mineral admixtures and polymer latex. Constr. Build. Mater. 168, 946–957. https://doi.org/10.1016/j.conbuildmat.2018.02.205.
Reischl, B., Raiteri, P., Gale, J.D., Rohl, A.L., 2019. Atomistic simulation of atomic force microscopy imaging of hydration layers on calcite, dolomite, and magnesite surfaces. J. Phys. Chem. C 123, 14985–14992. https://doi.org/10.1021/acs.jpcc.9b00939.
Richards, D., Milner, R.G., Huang, F., Festy, F., 2003. Tip-enhanced Raman microscopy: practicalities and limitations. J. Raman Spectrosc. 34, 663–667. https://doi.org/10.1002/jrs.1046.
Sader, J.E., Uchihashi, T., Higgins, M.J., Farrell, A., Nakayama, Y., Jarvis, S.P., 2005. Quantitative force measurements using frequency modulation atomic force microscopy theoretical foundations. Nanotechnology 16, S94–S101. https://doi.org/10.1088/0957-4484/16/3/018.
Saldi, G.D., Voltolini, M., Knauss, K.G., 2017. Effects of surface orientation, fluid chemistry and mechanical polishing on the variability of dolomite dissolution rates. Geochim. Cosmochim. Acta 206, 94–111. https://doi.org/10.1016/j.gca.2017.02.007.
Shao, F., Zenobi, R., 2019. Tip-enhanced Raman spectroscopy: principles, practice, and applications to nanospectroscopic imaging of 2D materials. Anal. Bioanal. Chem. 411, 37–61. https://doi.org/10.1007/s00216-018-1392-0.
Shao, H., Chang, J., Lu, Z., Luo, B., Grundy, J.S., Xie, G., et al., 2019. Probing anisotropic surface properties of illite by atomic force microscopy. Langmuir 35, 6532–6539. https://doi.org/10.1021/acs.langmuir.9b00270.
Shinato, K.W., Huang, F., Jin, Y., 2020. Principle and application of atomic force microscopy (AFM) for nanoscale investigation of metal corrosion. Corros. Rev. 38, 423–432. https://doi.org/10.1515/corrrev-2019-0113.
Siretanu, I., van den Ende, D., Mugele, F., 2016. Atomic structure and surface defects at mineral-water interfaces probed by in situ atomic force microscopy. Nanoscale 8, 8220–8227. https://doi.org/10.1039/c6nr01403h.
Sokolov, Y., Henderson, G.S., Wicks, F.J., 2000. Model dependence of AFM simulations in non-contact mode. Surf. Sci. 457, 267–272. https://doi.org/10.1016/S0039-6028(00)00384-8.
Songen, H., Reischl, B., Miyata, K., Bechstein, R., Raiteri, P., Rohl, A.L., et al., 2018. Resolving point defects in the hydration structure of calcite (10.4) with three-dimensional atomic force microscopy. Phys. Rev. Lett. 120, 116101 https://doi.org/10.1103/PhysRevLett.120.116101.
Songen, H., Jaques, Y.M., Spijker, P., Marutschke, C., Klassen, S., Hermes, I., et al., 2020. Three-dimensional solvation structure of ethanol on carbonate minerals. Beilstein J. Nanotechnol. 11, 891–898. https://doi.org/10.3762/bjnano.11.74.
Stark, R.W., Heckl, W.M., 2000. Fourier transformed atomic force microscopy tapping mode atomic force microscopy beyond the Hookian approximation. Surf. Sci. 457 (1), 219–228. https://doi.org/10.1016/S0039-6028(00)00378-2.

Strahlendorff, T., Dai, G., Bergmann, D., Tutsch, R., 2019. Tip wear and tip breakage in high-speed atomic force microscopes. Ultramicroscopy 201, 28–37. https://doi.org/10.1016/j.ultramic.2019.03.013.

Sun, W., Han, H., Sun, W., Wang, R., Wei, Z., 2022. Novel insights into the role of colloidal calcium dioleate in the flotation of calcium minerals. Miner. Eng. 175, 107274 https://doi.org/10.1016/j.mineng.2021.107274.

Suyantara, G.P.W., Hirajima, T., Miki, H., Sasaki, K., Yamane, M., Takida, E., et al., 2018. Selective flotation of chalcopyrite and molybdenite using H2O2 oxidation method with the addition of ferrous sulfate. Miner. Eng. 122, 312–326. https://doi.org/10.1016/j.mineng.2018.02.005.

Tadesse, B., Makuei, F., Albijanic, B., Dyer, L., 2019. The beneficiation of lithium minerals from hard rock ores: a review. Miner. Eng. 131, 170–184. https://doi.org/10.1016/j.mineng.2018.11.023.

Tessarolo, N., Wang, N., Wicking, C., Collins, I., Webb, K., Couves, J., et al., 2021. Identification of organic species with "double-sided tape" characteristics on the surface of carbonate reservoir rock. Fuel 288, 119627. https://doi.org/10.1016/j.fuel.2020.119627.

Toca-Herrera, J.L., 2019. Atomic force microscopy meets biophysics, bioengineering, chemistry, and materials science. ChemSusChem 12, 603–611. https://doi.org/10.1002/cssc.201802383.

Tong, Z., Liu, L., Yuan, Z., Liu, J., Lu, J., Li, L., 2021. The effect of comminution on surface roughness and wettability of graphite particles and their relation with flotation. Miner. Eng. 169, 106959 https://doi.org/10.1016/j.mineng.2021.106959.

Vijayraghavan, K., Gellineau, A.A., Wang, A., Butte, M.J., Melosh, N.A., Solgaard, O., 2013. High-bandwidth AFM probes for imaging in air and fluid. Microelectromech. Syst. 22, 603–612.

Wang, G., Ran, L., Xu, J., Wang, Y., Ma, L., Zhu, R., et al., 2021b. Technical development of characterization methods provides insights into clay mineral-water interactions: a comprehensive review. Appl. Clay Sci. 206, 106088 https://doi.org/10.1016/j.clay.2021.106088.

Wang, K., Taylor, K.G., Ma, L., 2021a. Advancing the application of atomic force microscopy (AFM) to the characterization and quantification of geological material properties. Int. J. Coal Geol. 247, 103852 https://doi.org/10.1016/j.coal.2021.103852.

Wang, R., Lu, Q., Sun, W., Lin, S., Han, H., Sun, W., et al., 2022. Flotation separation of apatite from calcite based on the surface transformation by fluorite particles. Miner. Eng. 176, 107320 https://doi.org/10.1016/j.mineng.2021.107320.

Wu, P., Zhang, H., J. G, 1998. The application of atomic force microscope to clay minerals. Adv. Earth Sci. 34–38. https://doi.org/10.11867/j.issn.1001-8166.1998.04.0351.

Xiao, L., Schultz, Z.D., 2018. Spectroscopic imaging at the nanoscale: technologies and recent applications. Anal. Chem. 90, 440–458. https://doi.org/10.1021/acs.analchem.7b04151.

Xiao, W., Zhao, H., Qin, W., Qiu, G., Wang, J., 2018. Adsorption mechanism of Pb2+ activator for the flotation of rutile. Minerals 8, 266. https://doi.org/10.3390/min8070266.

Xie, L., van Zyl, D., 2020. Distinguishing reclamation, revegetation and phytoremediation, and the importance of geochemical processes in the reclamation of sulfidic mine tailings: a review. Chemosphere 252, 126446. https://doi.org/10.1016/j.chemosphere.2020.126446.

Xing, Y., Xu, M., Gui, X., Cao, Y., Babel, B., Rudolph, M., et al., 2018. The application of atomic force microscopy in mineral flotation. Adv. Colloid Interface Sci. 256, 373–392. https://doi.org/10.1016/j.cis.2018.01.004.

Yang, J., Hatcherian, J., Hackley, P.C., Pomerantz, A.E., 2017. Nanoscale geochemical and geomechanical characterization of organic matter in shale. Nat. Commun. 8, 2179. https://doi.org/10.1038/s41467-017-02254-0.

Yi, H., Zhang, X., Jia, F., Wei, Z., Zhao, Y., Song, S., 2019. Competition of Hg2+ adsorption and surface oxidation on MoS2 surface as affected by sulfur vacancy defects. Appl. Surf. Sci. 483, 521–528. https://doi.org/10.1016/j.apsusc.2019.03.350.

Yuan, K., Starchenko, V., Lee, S.S., De Andrade, V., Gursoy, D., Sturchio, N.C., et al., 2019. Mapping three-dimensional dissolution rates of calcite microcrystals: effects of surface curvature and dissolved metal ions. ACS Earth Space Chem. 3, 833–843. https://doi.org/10.1021/acsearthspacechem.9b00003.

Yuan, Y., Zhan, W., Jia, F., Song, S., 2020. Multi edged molybdenite achieved by thermal modification for enhancing Pb(II) adsorption in aqueous solutions. Chemosphere 251, 126369. https://doi.org/10.1016/j.chemosphere.2020.126369.

Zhai, H., Zhang, W., Wang, L., Putnis, C.V., 2021. Dynamic force spectroscopy for quantifying single-molecule organo–mineral interactions. CrystEngComm 23, 11–23. https://doi.org/10.1039/d0ce00949k.

Zhang, H., Huang, J., Wang, Y., Liu, R., Huai, X., Jiang, J., et al., 2018. Atomic force microscopy for two-dimensional materials: a tutorial review. Opt. Commun. 406, 3–17. https://doi.org/10.1016/j.optcom.2017.05.015.

Zhang, L., Wang, Y., Miao, X., Gan, M., Li, X., 2019a. Geochemistry in geologic CO_2 utilization and storage: a brief review. advances in geo-energy. Research 3, 304–313. https://doi.org/10.26804/ager.2019.03.08.

Zhang, X., Jia, F., Yang, B., Song, S., 2017b. Oxidation of molybdenum disulfide sheet in water under in situ atomic force microscopy observation. J. Phys. Chem. C 121, 9938–9943. https://doi.org/10.1021/acs.jpcc.7b01863.

Zhang, X., Yi, H., Bai, H., Zhao, Y., Min, F., Song, S., 2017a. Correlation of montmorillonite exfoliation with interlayer cations in the preparation of two-dimensional nanosheets. RSC Adv. 7, 41471–41478. https://doi.org/10.1039/c7ra07816a.

Zhang, Z., Tan, Y., Dong, G., Yang, Z., 2012. Improvement on surface force apparatus and verification of DLVO theory in solution. Chem. Res. 23, 16–20. https://doi.org/10.14002/j.hxya.2012.03.007.

Zhang, Z., Cao, Y., Sun, L., Ma, Z., Liao, Y., 2019b. Interaction forces between scheelite and fluorite in calcium solution measured by atomic force microscopy. Appl. Surf. Sci. 486, 323–336. https://doi.org/10.1016/j.apsusc.2019.05.023.

Zhao, S., Li, Y., Wang, Y., Ma, Z., Huang, X., 2019. Quantitative study on coal and shale pore structure and surface roughness based on atomic force microscopy and image processing. Fuel 244, 78–90. https://doi.org/10.1016/j.fuel.2019.02.001.

Zhou, H., Tang, Y., Zhang, S., 2020. Advanced Spectroscopic Technique for the Study of Nanocontainers: Atomic Force Microscopy-infrared Spectroscopy (AFM-IR). Elsevier, pp. 7–17. https://doi.org/10.1016/b978-0-12-816770-0.00002-2.

Zhu, J., Sun, R.G., 2005. Introduction to atomic force microscope and its manipulation. Life Sci. Instrum. 22–26.

Zhu, Z., Yin, W., Wang, D., Sun, H., Chen, K., Yang, B., 2020a. The role of surface roughness in the wettability and floatability of quartz particles. Appl. Surf. Sci. 527, 146799 https://doi.org/10.1016/j.apsusc.2020.146799.

Zhu, Z., Wang, D., Yang, B., Yin, W., Ardakani, M.S., Yao, J., et al., 2020b. Effect of nano-sized roughness on the flotation of magnesite particles and particle-bubble interactions. Miner. Eng. 151, 106340 https://doi.org/10.1016/j.mineng.2020.106340.

Zhu, Z., Yin, W., Han, H., Cao, S., Yang, B., Wang, D., 2020c. Investigation on the influence of surface roughness on magnetite flotation from the view of both particle-particle and bubble-particle interactions. Colloids Surf. A Physicochem. Eng. Asp. 595, 124681 https://doi.org/10.1016/j.colsurfa.2020.124681.

Zou, W., Gong, L., Pan, M., Zhang, Z., Sun, C., Zeng, H., 2020. Effect of salinity on adsorption and interaction forces of hydrophobically modified polyacrylamide on silica and alumina surfaces. Miner. Eng. 150, 106280 https://doi.org/10.1016/j.mineng.2020.106280.